Hindawi Publishing Corporation
Journal of Chemistry
Volume 2015, Article ID 932616, 11 pages
http://dx.doi.org/10.1155/2015/932616

Research Article

Design of Pd-Based Bimetallic Catalysts for ORR: A DFT Calculation Study

Lihui Ou

College of Chemistry and Chemical Engineering, Hunan University of Arts and Science, Changde, Hunan 415000, China

Correspondence should be addressed to Lihui Ou; oulihui666@126.com

Received 14 May 2015; Revised 14 July 2015; Accepted 15 July 2015

Academic Editor: Demeter Tzeli

Developing Pd-lean catalysts for oxygen reduction reaction (ORR) is the key for large-scale application of proton exchange membrane fuel cells (PEMFCs). In the present paper, we have proposed a multiple-descriptor strategy for designing efficient and durable ORR Pd-based alloy catalysts. We demonstrated that an ideal Pd-based bimetallic alloy catalyst for ORR should possess simultaneously negative alloy formation energy, negative surface segregation energy of Pd, and a lower oxygen binding ability than pure Pt. By performing detailed DFT calculations on the thermodynamics, surface chemistry and electronic properties of Pd-M alloys, Pd-V, Pd-Fe, Pd-Zn, Pd-Nb, and Pd-Ta, are identified theoretically to have stable Pd segregated surface and improved ORR activity. Factors affecting these properties are analyzed. The alloy formation energy of Pd with transition metals M can be mainly determined by their electron interaction. This may be the origin of the negative alloy formation energy for Pd-M alloys. The surface segregation energy of Pd is primarily determined by the surface energy and the atomic radius of M. The metals M which have smaller atomic radius and higher surface energy would tend to favor the surface segregation of Pd in corresponding Pd-M alloys.

1. Introduction

Fuel cells have received much attention in recent years as the global effort to reduce our reliance on fossil fuels has increased. In particular, low-temperature proton exchange membrane fuel cells (PEMFCs) possess great potential as substitutes for conventional combustion engines in future mobile applications, which can efficiently convert chemical energy into electrical energy. However, the development of PEMFCs is severely hampered by the fact that the oxygen reduction reaction (ORR) is slow, even when using Pt as a catalyst. The sluggish kinetics of the ORR requires a substantial amount of this precious metal within their cathodes in real electrochemical systems, which has limited the scaling-up of corresponding renewable energy technologies. Therefore, the PEMFCs still leave room for reducing cost and improving efficiency that could be achieved by finding more active and stable electrocatalytic cathode catalysts for ORR. Because Pt is expensive and scarce, alloys have attracted interest in the request to develop advanced electrocatalysts in recent years [1–4]. Several Pt alloys, such as Pt-Fe, Pt-Co, Pt-Ni, and Pt-Cu [5–14], are considerably more active than Pt and have been studied extensively toward advanced ORR electrocatalysts. For example, Stamenkovic et al. found that on Pt_3Ni the ORR is 90 times faster than on pure Pt [8]. Alloying Pt with nonnoble transition metals, Fe, Co, and Cu, can increase the catalytic activity and the stability of these catalysts, where their Pt-based alloy catalysts have been reported to be 2–10 times more active than polycrystalline Pt for the ORR [6, 9, 13, 15–22]. However, one of the major drawbacks of PEMFCs commercialization is the high cost of Pt-based catalysts. Thus, alternative cost-effective catalysts must be developed to eliminate the Pt-based ones. Recent studies on ORR electrocatalysis have attempted to replace Pt with less-expensive materials.

In recent years, some Pd-M (M is transition metals) alloys have been used as ORR electrocatalysts [23–30], in which alloying with Fe and Co was found to increase strongly the ORR electrocatalytic activity of Pd. This represents significant progress in the research on non-Pt ORR catalysts for PEMFCs. For example, Adzic [28, 29] studied Pd-M alloy electrocatalysts and found that Pd-Fe and Pd-Co alloys become very active for ORR, and Pd atoms segregate to

the surface to form a pure Pd skin on bulk alloys. The results showed that the active ORR electrocatalysts can be devised without Pt, and their activity can surpass those of pure Pt electrocatalysts [29]. Further enhancement of the ORR catalytic activity and stability of Pd is of considerable interest, and replacing Pt with the less-expensive metal Pd alloy can considerably decrease the operational costs, thereby facilitating the faster and broader application of PEMFCs. In the search for improved alloy catalyst materials, different strategies and schemes have been used, from experimental high-throughput catalyst screen [31] to the study of idealized model systems [8]. But to date only limited efforts have been made to use computational techniques based on density functional theory (DFT) to screen for improved ORR catalysts [32]. The pace of materials discovery for alloy electrocatalysts could be accelerated in principle by the development of efficient computational screening methods. Some studies have proposed thermodynamic guidelines for design of Pd-based alloy electrocatalysts for ORR. For example, Bard et al. [30, 33, 34] suggested that, for Pd-M alloys, the site for O–O bond breaking is constituted by the transition metal M and then formed O_{ads} migrates to hollow sites formed by Pd atoms, where it is easily reduced to water. Based on this mechanism, the alloy surface should compose of a relatively reactive metal such as Co, and the atomic ratio of this transition metal should be 10% to 20% so that sufficient sites exist for reactions of O–O bond breaking on M and for O_{ads} reduction at hollow sites dominated by Pd atoms. Wang and Balbuena [35, 36] proposed a similar thermodynamic guideline for design of Pd-based bimetallic alloy catalysts. For Pd with fully occupied valence d-orbitals, alloying with transition metals such as Co with unoccupied valence d-orbitals significantly reduces the Gibbs free energy both for the first charge-transfer step and for the steps involving the reduction of intermediates. Although these studies have convincingly showed that first-principles catalyst design is now a reality for the ORR and corresponding progress has been made in this respect, these arguments for ORR electrocatalysis on Pd-based bimetallic surfaces cannot explain the relatively good activity and stability of Pd-M alloys in acidic medium [37]. On the other hand, the Pd-enriched skin can account for both the good activity and stability of these alloys [38–40]. Hence, a fully DFT-based, high-throughput, computational design and screening of Pd-based alloy catalysts has yet to be realized, and further development of screening schemes is still necessary for design of Pd-based bimetallic catalysts.

As we all know, the ORR occurs in electrochemical environments under conditions of high electrode potential and is, thus, expected to be susceptible to the stability issues mentioned above. Indeed, recent reports have highlighted the importance of stability considerations in the identification of improved ORR catalysts [8, 41]. Pd materials are known to be kinetically stable in electrochemical systems over relatively long periods of operation [42, 43]. It is also one of the metallic elements that are stable under the high potentials and acidic conditions of a PEMFC [44]. Additionally, core-shell particles that possess an inexpensive core surrounded by a Pd shell are extensively discussed as promising PEMFC catalyst materials and can account for both the good activity and the stability of Pd-based alloys at present. However, the stability issues have almost been not considered in previous computational design and screen of alloy catalysts based on DFT. Therefore, in the present paper we will focus our attention on Pd-based alloy catalysts that could form a protective Pd shell on the topmost surface layer and that possess a high tendency to segregate, a property closely dependent on the surface segregation energy.

As electrocatalytic reactions on catalysts are far too complex for a complete theoretical description, the complexity is first reduced. Consequently, in the present study, we restrict our calculations to close packed surfaces and, in this contribution, we search for a DFT-based, computational catalyst screening procedure including the adsorption energy of O atom, the alloy formation energy, and the surface segregation energy of Pd that are considered sufficiently able to predict the catalytic activity and stability of alloy catalysts. The overall goal is to find alloys of the composition Pd_3M (M is transition metals) with improved ORR activity and stability. We illustrate the use of this scheme on the ORR and successfully use these strategies to identify several promising new catalysts for this reaction, and some alloy catalysts have been synthesized and tested experimentally and show improved ORR performance compared with pure Pt. Although our results were not always quantitatively accurate, the conclusions on trends were reasonably accurate qualitatively because the present experimental phenomenon of the ORR confirmed the computational screening results.

2. Models and Methods

Calculations were carried out based on the periodic DFT slab approach by using the generalized gradient approximation with the Perdew-Burke-Ernzerhof exchange correlation functional [45]. The nuclei and core electrons were described by using PAW potentials [46]. The Kohn-Sham equations were solved self-consistently by using a plane-wave basis set. A kinetic energy cutoff of 26 Ry and a charge-density cutoff of 260 Ry were used to make the plane-wave basis set finite. The Fermi surface has been treated by the smearing technique of Methfessel-Paxton with a parameter of 0.02 Ry [47]. All calculations in this study have been implemented by using the PWSCF codes included in the Quantum ESPRESSO distribution [48], while figures of the chemical structures were produced with the XCRYSDEN graphical package [49–51].

Crystal structure of Pd-based alloys is calculated with $L1_2$ cubic system structure in which the stoichiometric ratio is 3 : 1 [52], in which the Pd atoms occupy the face-centered positions and the M (M is 3d, 4d, and 5d transition metals) atoms are located at the corners in the unit cell. For each Pd_3M structure, the lattice constant was obtained after a bulk optimization. In all calculations, the (2×2) five-layer fcc(111) slabs with theoretical equilibrium lattice constant to model the $Pd_3M(111)$ surface were used. In the super cell, each slab layer contains 3 Pd atoms and 1 M atom.

The segregation structures were reached by exchanging M atoms at the first layer and Pd atoms at the second layer. Therefore, the topmost layer is fully covered by Pd atoms and the second layer contains 50% Pd atoms for each Pd segregation structure. A (4×4) uniformly shifted k-mesh

was used to describe the first Brillouin-zone for (2 × 2) slab. Vacuum layers 16 Å in thickness were added above the top layer of slabs in all cases, which is sufficiently large to ensure that the interactions between repeated slabs are negligible. In the slab calculations, the structure of the bottom two layers of the slab was fixed at the theoretical bulk positions, whereas the geometry of the top three layers and all other structural parameters on a (2 × 2) five-layer slab was allowed to fully relax to minimize the total energy of the system. The criteria for the total energy and the Cartesian force components acting on each atom convergence used were within 10^{-5} Ry and below 10^{-3} Ry/Bohr with regard to structural optimization, respectively.

The d-band center of surface atoms, ε_d, is a key parameter that influence surface adsorption characteristics [53, 54]. Therefore, ε_d was calculated in various catalytic materials, and the relationship between the values of ε_d and the adsorption energy of O atom was examined. The d-band center was calculated as the first moment of the projected d-band density of states on the surface atoms referenced to the Fermi level.

3. Design Schemes for Alloy Catalysts of ORR

3.1. Stability Descriptor of Pd-Based Bimetallic Catalysts. It could be imagined that formation of Pd-based bimetallic catalysts with Pd surface segregated structure can be divided into two stages. Primarily, bulk alloys must be formed by the liquid phase or solid phase reactions between Pd and transition metals M. Thus, the fact that formation energies, ΔE_{alloy}, of the alloys of reaction $n\text{Pd} + m\text{M} \rightarrow \text{Pd}_n\text{M}_m$ are negative is required. Otherwise, separate phase is formed between Pd and transition metals M. ΔE_{alloy} is calculated by the formula $\Delta E_{\text{alloy}} = E(A_xB_{1-x}; a) - xE_A(a_A^0) - (1 - x)E_B(a_B^0)$, where $E(A_xB_{1-x}; a)$ is the total energy of the alloy, $E_A(a_A^0)$ and $E_B(a_B^0)$ are the total energy of constituents A and B under equilibrium lattice constant, respectively. Then, there is surface segregation of interior Pd atoms to form Pd segregated surface via some special processes such as high temperature annealing or surface inducing adsorption. In general, the surface segregation energy, ΔE_{segr}, is the energy of moving an atom from the interior to the surface of a crystal. In this work, it is defined as the difference of total free energies between the slabs with the Pd surface segregated structure and that with the bulk structure. Negative surface segregation energy indicates that the interior Pd atoms are able to segregate to the surface, while positive segregation energy suggests that no Pd segregation occurs on the surface. Although the structure of Pd segregated surface can be achieved by depositing Pd on transition metals or dealloying of Pd-based alloy catalysts, this do not influence the fact that surface segregation energy ΔE_{segr} is a negative act as stability descriptor of alloy catalysts with Pd segregated surface.

3.2. Activity Descriptor of Pd-Based Bimetallic Catalysts. In our previous study on ORR mechanisms [55], the results indicated that the protonation of adsorbed O atom to form OH is the rate-determining step (rds) on the Pd(111) surface; such finding about the rds of ORR indicates that the ORR activity of the Pd segregated surface can be assessed by their binding ability to oxygenated species and Pd-based catalysts that more weakly bind atomic oxygen than pure Pt may have better ORR activity. It has been well-established in the literature that Pd and Pt are somewhat too oxophilic so that the surface oxygenated species formed from dissociation of O_2 tend to block the surface sites for ORR [56]. Thus, oxygen adsorption energy can be a good descriptor for the ORR catalytic activity of Pd-based bimetallic alloys. If the adsorption energy of O atom on stable alloy catalysts with Pd segregated surface is close to or slightly weaker than that of pure Pt, the alloy catalysts should have enhanced ORR performance compared with pure Pt. The adsorption energies are calculated with the energies of the bare $Pd_3M(111)$ slab (E_{slab}) with Pd segregated surface and the isolated oxygen atom E_{O} as the references according to

$$E_{\text{ads}}^{\text{O}} = E_{\text{total}} - E_{\text{slab}} - E_{\text{O}}, \quad (1)$$

where E_{total} refers to the total energies of the optimized slab/O system.

To sum up, three criteria should be met simultaneously for ideal Pd-based ORR alloy catalysts: (1) $\Delta E_{\text{alloy}} < 0$; (2) $\Delta E_{\text{segr}} < 0$; (3) $\Delta E_{\text{O}} = E_{\text{alloy}}^{\text{O}} - E_{\text{Pt}}^{\text{O}} > 0$. Therefore, we applied DFT method to calculate above mentioned three criteria for alloy catalysts based on Pd_3M model and then expect that possible ORR catalysts with high activity and stability could be revealed theoretically.

4. Results and Discussion

According to the sequence of periodic table of elements, the DFT-calculated lattice constants (a) and the values for three criteria of various Pd_3M alloys are shown in Tables 1, 2, and 3 when M is 3d, 4d, and 5d transition metals, respectively. Valence electron configuration (VEC) of transition metals M is also given.

4.1. Stability Analysis of Pd-Based Bimetallic Catalysts. According to the formation energies of Pd_3M alloys in Tables 1, 2, and 3, it can be predicted that 3d transition metals Sc, Ti, V, Cr, Mn, Fe, Cu, and Zn, 4d transition metals Nb, Mo, Ru, and Rh, and 5d transition metals Ta, W, Re, Ir, and Pt can form stable alloys with Pd since the formation energy ΔE_{alloy} of these Pd-based bimetallic alloys is negative.

To ascertain the effect of electronic structure on stability of Pd-based alloys, the variation trend of the DFT-calculated ΔE_{alloy} of Pd_3M (M is 3d, 4d, and 5d transition metals) alloys with the valence electrons number (sums of outmost s and d electrons) of M is shown in Figure 1. The results show that the values of ΔE_{alloy} become more and more positive firstly and then become more and more negative as valence electrons number increases. There are the most positive ΔE_{alloy} in Pd_3Co (valence electrons number of Co is 9), Pd_3Ru (valence electrons number of Ru is 8), and Pd_3Re site (valence electrons number of Re is 7) for the alloys that formed by Pd and 3d, 4d, and 5d transition metals, respectively, which are approximately in the center of periodic table of elements. Therefore, the fact that whether they can

Table 1: The DFT calculated lattice constants, formation energies, ΔE_{alloy} (eV), surface segregation energies of Pd, ΔE_{segr} (eV) for various Pd_3M (M is 3d transition metals) alloys and adsorption energies difference of O atom between Pd-segregated $Pd_3M(111)$ and Pt(111) surface, ΔE_O (eV).

Alloys	Pd_3Sc	Pd_3Ti	Pd_3V	Pd_3Cr	Pd_3Mn	Pd_3Fe	Pd_3Co	Pd_3Ni	Pd_3Cu	Pd_3Zn
VEC	$3d^14s^2$	$3d^24s^2$	$3d^34s^2$	$3d^54s^1$	$3d^54s^2$	$3d^64s^2$	$3d^74s^2$	$3d^84s^2$	$3d^{10}4s^1$	$3d^{10}4s^2$
a (Å)	4.02	3.94	3.92	3.90	3.92	3.91	3.89	3.89	3.91	3.93
ΔE_O (eV)	0.31	0.44	0.44	0.32	0.32	0.40	0.34	0.24	0.16	0.30
ΔE_{alloy} (eV)	−0.92	−0.67	−0.30	−0.20	−0.28	−0.20	0.035	0.025	−0.084	−0.33
ΔE_{segr} (eV)	1.26	0.76	−0.62	0.13	0.19	−0.22	−0.45	−0.25	0.0027	−0.086

Table 2: The DFT calculated lattice constants, formation energies, ΔE_{alloy} (eV), surface segregation energies of Pd, ΔE_{segr} (eV) for various Pd_3M (M is 4d transition metals) alloys, and adsorption energies difference of O atom between Pd-segregated $Pd_3M(111)$ and Pt(111) surface, ΔE_O (eV).

Alloys	Pd_3Y	Pd_3Zr	Pd_3Nb	Pd_3Mo	Pd_3Ru	Pd_3Rh	Pd_3Ag	Pd_3Cd
VEC	$4d^15s^2$	$4d^25s^2$	$4d^45s^1$	$4d^55s^1$	$4d^75s^1$	$4d^85s^1$	$4d^{10}5s^1$	$4d^{10}5s^2$
a (Å)	4.14	4.04	3.99	3.97	3.93	3.94	4.01	4.03
ΔE_O (eV)	0.18	0.35	0.46	0.31	0.10	0.04	−0.05	0.13
ΔE_{alloy} (eV)	−0.92	−0.84	−0.40	−0.025	0.17	0.083	−0.027	−0.32
ΔE_{segr} (eV)	2.45	1.99	−0.59	−2.17	−1.10	−0.49	0.24	0.44

Table 3: The DFT calculated lattice constants, formation energies, ΔE_{alloy} (eV), surface segregation energies of Pd, ΔE_{segr} (eV) for various Pd_3M (M is 5d transition metals) alloys, and adsorption energies difference of O atom between Pd-segregated $Pd_3M(111)$ and Pt(111) surface, ΔE_O (eV).

Alloys	Pd_3Ta	Pd_3W	Pd_3Re	Pd_3Ir	Pd_3Pt	Pd_3Au
VEC	$5d^36s^2$	$5d^46s^2$	$5d^56s^2$	$5d^76s^2$	$5d^96s^1$	$5d^{10}6s^1$
a (Å)	3.98	3.97	3.94	3.94	3.97	4.02
ΔE_O (eV)	0.12	0.41	0.48	0.00	−0.06	−0.07
ΔE_{alloy} (eV)	−0.37	−0.051	0.23	0.15	−0.016	−0.050
ΔE_{segr} (eV)	−0.65	−2.40	−3.07	−0.80	−0.037	0.41

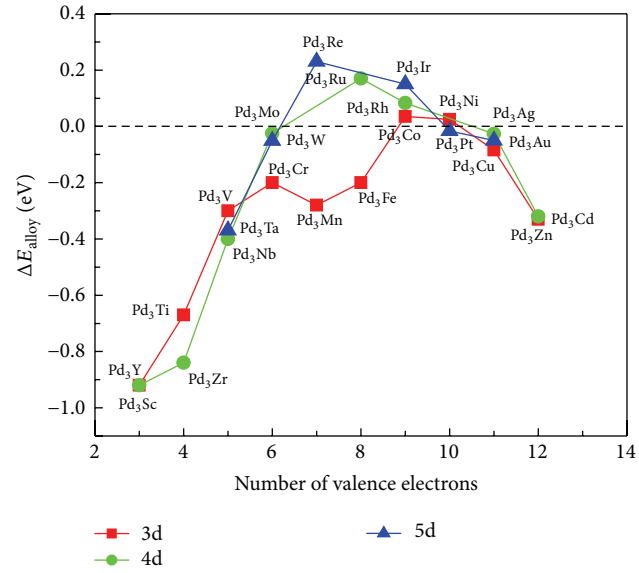

Figure 1: The relationship between the calculated formation energies of Pd_3M alloys, ΔE_{alloy}, and number of valence electrons.

form stable alloys between Pd and transition metals is related to valence electrons number of transition metals. This should be due to ΔE_{alloy} values that can be affected by the electronic interaction between Pd and transition metals M. For metals which have very different valence electrons numbers from that of Pd, the electronic interaction should be strong due to the large difference in electronegativity. This may be the origin of the largely negative ΔE_{alloy} for alloys of Pd with transition metals M.

Relation between the DFT-calculated segregation energy, ΔE_{segr}, of Pd in Pd_3M alloys and the valence electrons number of M is shown in Figure 2. For 3d transition metals, the ΔE_{segr} in Pd_3M alloys exhibit an oscillating variation with increasing the valence electrons number as moving from the left to right in the periodical table. The ΔE_{segr} for 4d and 5d metals show first decrease then increase with increasing valence electrons number. There are the most negative ΔE_{segr} in Pd_3V and Pd_3Co (valence electrons number of V and Co is 5 and 9, resp.), Pd_3Mo (valence electrons number of Mo is 6), and Pd_3Re site (valence electrons number of Re is 7) when alloying Pd with 3d, 4d, and 5d transition metals, respectively, which are also approximately in the center of periodic table of elements. This should be also due to ΔE_{segr} values that can be affected by the electronic interaction between Pd and M. For metals which have very different valence electrons numbers from that of Pd, the electronic interaction should be strong due to the large difference in electronegativity [57]. This may be also the origin of the largely negative ΔE_{segr} for alloys of Pd with transition metals. Thus, we may conclude that electronic interactions play the important role in determining the alloy formation energy and segregation energy of Pd of Pd-based bimetallic alloys for ORR.

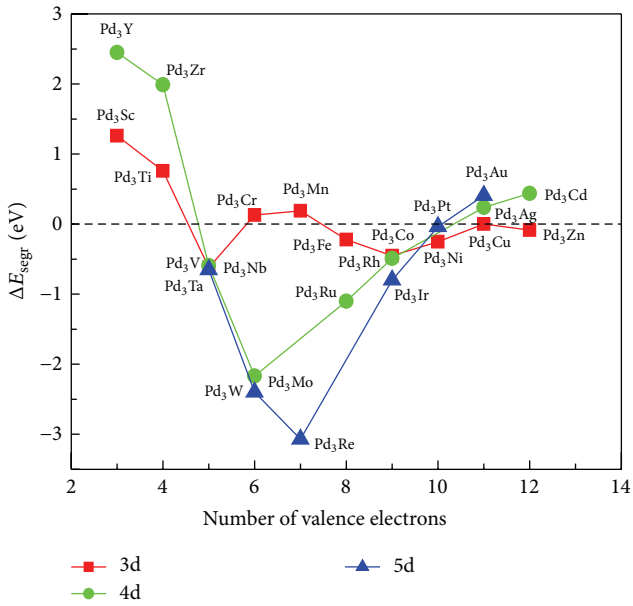

FIGURE 2: The relationship between the calculated segregation energy (ΔE_{segr}) of Pd_3M alloys and number of valence electrons.

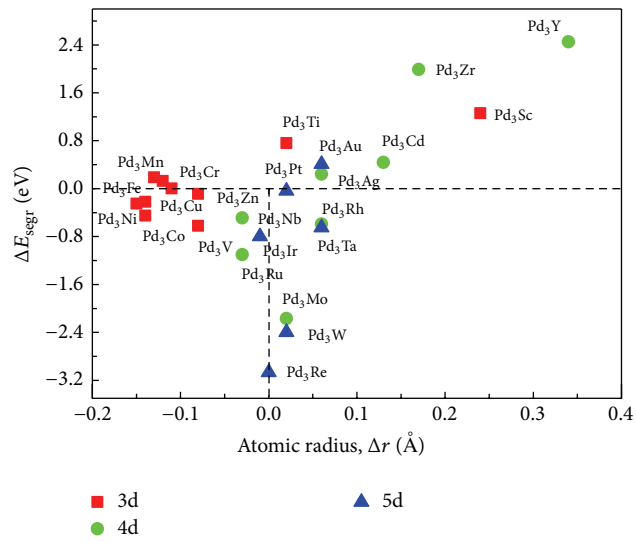

FIGURE 3: Plots of DFT-calculated segregation energy (ΔE_{segr}) of Pd in Pd_3M alloys as functions of atomic radii of alloying metals (M). Atomic radii are given with respect to that of Pd; that is, $\Delta r = r(M) - r(Pd)$.

According to the criteria of $\Delta E_{segr} < 0$, Pd-V, Pd-Fe, Pd-Co, Pd-Ni, Pd-Zn, Pd-Nb, Pd-Mo, Pd-Ru, Pd-Rh, Pd-Ta, Pd-W, Pd-Re, Pd-Ir, and Pd-Pt alloys are possible to form Pd segregated surface by surface segregation of Pd. It has been widely reported experimentally and theoretically that surface segregation is primarily determined by the surface energy and the atomic size [58, 59]. Metal atoms with larger radii and lower surface energies usually tend to segregate to the surface. The correlation between ΔE_{segr} and both the M metallic radius r [60] and the experimental surface energy E_{surf} [61] can be found in Figures 3 and 4, respectively. One can find that no matter when 3d, 4d, or 5d metals are the alloying elements, Pd is predicted to segregate to the surface for those metals with higher E_{surf} than Pd except for the Ti and Cr. This demonstrates that Pd surface segregation can be mainly determined by the surface energy. M with more positive E_{surf} than Pd does not always correspond to a negative ΔE_{segr} in the corresponding Pd_3M alloy since values of ΔE_{segr} are also affected by atomic radius, such as Ti and Cr, which have atomic radii close to and lower than that of Pd, respectively. As far as we know, segregating Pd atom to the surface alleviates the large strain in the alloy and thus decreases the total energy. This leads to the conclusion that the atomic size may be also an important factor for surface segregation. It can be found that Pd tends to segregate to the surface for those metals with atomic radii smaller than Pd except for Mn and Cr. In some cases, it can even determine the direction of surface segregation. For example, Pd-Ti, Pd-Cu, and Pd-Zn alloys, in which Ti possesses a much slight larger atomic radius than Pd, are still predicted to have positive segregation energy of Pd although its slightly higher surface energies than Pd, Cu, and Zn possess much smaller atomic radii than Pd and are still predicted to have a slight trend of Pd surface segregation, in spite of their very low

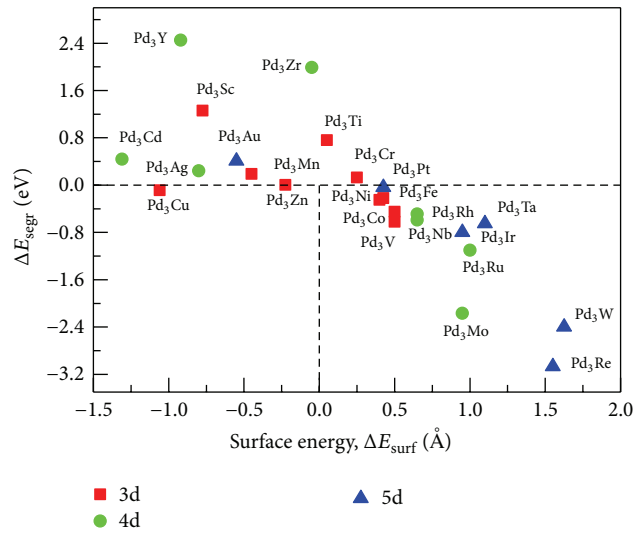

FIGURE 4: Plots of DFT-calculated segregation energy (ΔE_{segr}) of Pd in Pd_3M alloys as functions of experimental surface energies of alloying metals (M). Surface energies are given with respect to that of Pd; that is, $\Delta E_{surf} = E_{surf}(M) - E_{surf}(Pd)$.

E_{surf} relative to that of Pd. As mentioned above, metal Cr alloy has higher surface energy and lower atomic radius than Pd. However, Pd_3Cr alloy has positive segregation energy of Pd, indicating that electronic interaction may play the major role in determining the segregation energy of Pd in Pd_3Cr alloy. For other metals M, such as 3d transition metal, Sc, 4d transition metals, Y, Zr, Ag, and Cd, 5d transition metal, Au, which have larger atomic radii and lower surface energy than

Pd, alloys of Pd_3Sc, Pd_3Y, Pd_3Zr, Pd_3Ag, Pd_3Cd, and Pd_3Au exhibit considerably positive segregation energy ΔE_{segr}. Thus, it will be difficult for Pd_3Sc, Pd_3Y, Pd_3Zr, Pd_3Ag, Pd_3Cd, and Pd_3Au alloys to form Pd surface segregated structure. The segregation energy ΔE_{segr} of Pd in Pd_3Mn alloy is positive and mainly determined by its surface energy because 3d transition metal Mn has smaller atomic radius and lower surface energy than Pd. Since 4d transition metal, Mo, and 5d transition metals W, Re, Ir, and Pt mostly have similar atomic radii to Pd, values of segregation energy ΔE_{segr} for the Pd_3Mo, Pd_3W, Pd_3Re, Pd_3Ir, and Pd_3Pt alloys are mainly determined by their surface energy. W and Re especially have much more positive surface energy than Pd. Therefore, both of those alloys exhibit considerably negative segregation energy ΔE_{segr}.

To form a stable Pd surface segregated structure in Pd-M bimetallic alloys, it is necessary that both corresponding ΔE_{alloy} and ΔE_{segr} are negative. Otherwise, separate phase may tend to be formed between Pd and transition metals M. As shown in Figure 5, alloys of Pd with 3d transition metals V, Fe, and Zn simultaneously have negative ΔE_{alloy} and ΔE_{segr}. Alloys of Pd with early 4d transition metals have negative ΔE_{alloy} but positive ΔE_{segr}, while those with late 4d transition metals have negative ΔE_{segr} but positive ΔE_{alloy}. Only middle 4d transition metals such as Nb and Mo can form stable alloys with Pd, which simultaneously have negative ΔE_{alloy} and ΔE_{segr}. Thus, they should be able to form stable Pd surface segregated. Among Pd-5d alloys, Pd-Ta and Pd-W alloys simultaneously have negative ΔE_{alloy} and ΔE_{segr}. Thus, it is expected that Pd, Ta, and W could form stable alloys with Pd surface segregated structure.

The segregation process of Pd was also simulated in systems containing atomic oxygen adsorbed in the fcc (without transition metal atoms) and hcp (with a transition metal atom on the no Pd-segregated surface) positions, respectively. The most stable adsorption site for atomic oxygen is fcc on the Pd-segregated surface, and the differences of adsorption energy between fcc and hcp sites are relatively small. However, on no Pd-segregated surfaces, the differences of adsorption energy are large between both sites. Therefore, it is important to include the hcp case in the evaluation of surface segregation of Pd. The DFT-calculated surface segregation energies of Pd, ΔE_{segr}, for various Pd_3M (M is 3d, 4d, and 5d transition metals) alloys in systems containing atomic oxygen adsorbed in the fcc and hcp positions are given in Table 4. The results showed that the segregation energies of Pd change when atomic oxygen adsorbs in fcc site, but the segregation trend of Pd is almost not changed compared to the clean surfaces. It is noticeable that in the hcp site the segregation behavior of Pd in most Pd_3M alloys turns into nonsegregation (large position value of the segregation energy). It is observed that the presence of oxygen in hcp position causes the largest change in segregation energy of Pd, even leading to the reversion of segregation trends of Pd. It may be due to the fact that the high oxygen philicity of some M transition metal elements prohibit the surface segregation of Pd. Although the presence of oxygen in hcp position can revert the segregation behavior of Pd, strong adsorbed oxygenated species in hcp site may cause surface poisoning, which is unfavorable for ORR.

Table 4: The DFT calculated surface segregation energies of Pd, ΔE_{segr} (eV) for various Pd_3M (M is 3d, 4d, and 5d transition metals) alloys in systems containing atomic adsorbed in the fcc and hcp positions.

Pd_3M	fcc	hcp	Pd_3M	fcc	hcp	Pd_3M	fcc	hcp
Pd_3Sc	1.86	3.19	Pd_3Cu	0.16	0.19	Pd_3Ag	0.27	−0.16
Pd_3Ti	0.59	3.78	Pd_3Zn	0.18	0.27	Pd_3Cd	0.54	0.26
Pd_3V	−0.082	2.48	Pd_3Y	2.86	3.81	Pd_3Ta	−0.84	3.84
Pd_3Cr	0.50	2.06	Pd_3Zr	1.62	4.66	Pd_3W	−2.93	1.50
Pd_3Mn	0.57	1.32	Pd_3Nb	−0.83	3.53	Pd_3Re	−3.52	−0.86
Pd_3Fe	−0.068	1.01	Pd_3Mo	−2.42	−1.02	Pd_3Ir	−1.16	−0.23
Pd_3Co	−0.36	0.55	Pd_3Ru	−1.35	−0.17	Pd_3Pt	−0.22	−0.22
Pd_3Ni	−0.11	0.39	Pd_3Rh	−0.61	−0.11	Pd_3Au	0.30	−0.28

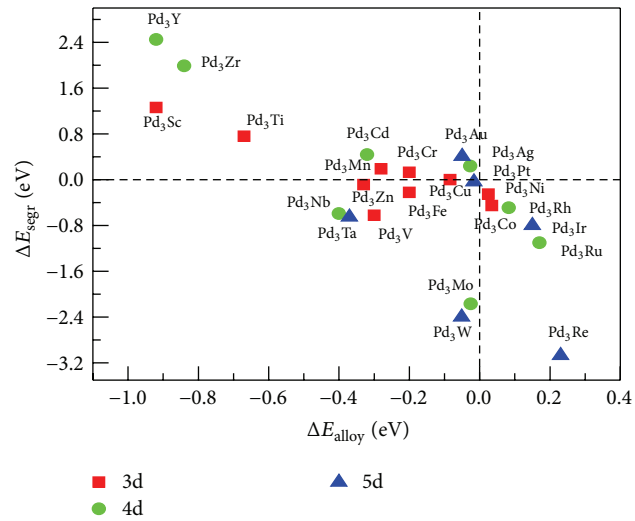

Figure 5: Relation between the DFT-calculated segregation energy (ΔE_{segr}) of Pd and formation energies in Pd_3M alloys: stability analysis.

In recent study conducted by Ramírez-Caballero and coworkers [62], DFT was used to evaluate the surface segregation of Pt, and two groups of cores are investigated, namely, a monolayer Pt over monometallic or bimetallic core. It was found that some 4d and 5d pure cores may serve as stable cores, and bimetallic Pd_3X cores could enhance the stability of the surface Pt atoms both in vacuum and under adsorbed oxygen. Our present studies also give similar results for the surface segregation of Pd. It can be observed that Pd still can segregate to surface when Pd alloys with 4d transition metals Mo, Ru, and Rh and 5d transition metals Re, Ir, Pt, and Au, even when oxygen adsorbs in hcp site, as shown in Table 4. Simultaneously, both of our present and previous studies from Ramírez-Caballero and coworkers all showed that surface segregation can be primarily determined by the surface energy and the atomic size, and metal atoms with larger radii and lower surface energies usually tend to segregate to the surface regardless of being the segregation process of Pd or Pt.

4.2. ORR Catalytic Activity Analysis of Pd-Based Bimetallic Catalysts. In this section, the adsorption energies of O atom are calculated on the all Pd-based bimetallic catalysts for comparison although some alloys cannot form stable Pd surface segregated structures. As shown in Tables 1, 2, and 3, the DFT-calculated O adsorption energies on Pd-segregated Pd-Sc, Pd-Ti, Pd-V, Pd-Cr, Pd-Mn, Pd-Fe, Pd-Co, Pd-Ni, Pd-Cu, Pd-Zn, Pd-Y, Pd-Zr, Pd-Nb, Pd-Mo, Pd-Ru, Pd-Rh, Pd-Ag, Pd-Cd, Pd-Ta, Pd-W, and Pt-Re alloys are more positive than that on pure Pt, indicating that these alloy catalysts may have enhanced ORR performance compared with pure Pt.

In order to verify d-band center model that Hammer and Nørskov proposed, that is, the interaction between surface atoms of metal and adsorbates weakens as downshift of ε_d, there is an approximate linear relationship between adsorption energy and ε_d [53, 54]. The relationship between O adsorption energies and ε_d is given in Figure 6. For all alloys considered in the present study, they mostly have E^{O}_{alloy} values which are close to or more positive than that on the pure Pt surface except for Pd_3Ag, Pd_3Ir, Pd_3Pt, and Pd_3Au alloys. Based on the volcano model of the ORR activity versus E^{O}_{alloy} values [56], E^{O}_{alloy} values of alloy surfaces with segregated structure are more positive than that for the pure Pt surface within 0.50 eV; the ORR activity would be close or superior to that of pure Pt. Thus, the Pd-based bimetallic alloys falling between two dash lines in Figure 6 will be potential ORR electrocatalysts. Meanwhile, it can be observed from Figure 6 that the calculated ΔE_O values between Pd_3M and Pt roughly linearly correlated with the calculated ε_d differences between Pd-segregated Pd_3M and Pd. In general, more negative $\Delta\varepsilon_d$ corresponds to more positive ΔE_O, indicating that adsorption characteristics of O on the Pd_3M alloy surfaces meet approximately the abovementioned d-band center model. Therefore, ε_d also could be a significant parameter for design of Pd-based alloy catalysts.

To understand the effect of the alloying elements on the electronic structure of the Pd segregated surface, the relationship between the calculated d-band center, ε_d, and number of valence electrons in M is shown in Figure 7. The results show that $\Delta\varepsilon_d$ values first decrease and then increase as the number of valence electrons of alloy elements (M) increase from the left to right in the periodical table when M is 3d or 4d transition metals and there is V-shaped change of $\Delta\varepsilon_d$ values, whereas, for 5d transition metals, the calculated $\Delta\varepsilon_d$ values linearly correlated with the number of valence electrons of alloy elements.

Alloying elements M may be able to affect the electronic structures of the Pd segregated surface by lattice strain (strain effect) or electronic interaction (ligand effect). In general, compressive strain results in downshift of d-band center, ε_d; namely, the value of ε_d becomes more negative than that of the pure Pd. As shown in Figure 8, the values of d-band center, ε_d, as a function of the optimized lattice constant (a) values are given. One can see from Figure 8 that compressive strain leads to downshift of d-band center, ε_d, as compared with that of pure Pd among all Pd_3M alloys that we have considered, regardless of M being 3d, 4d, or 5d transition metals; tensile strain results in upshift of d-band

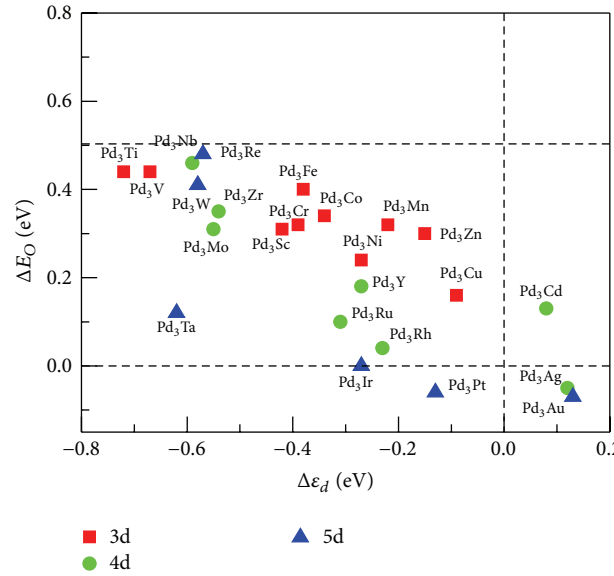

FIGURE 6: The relationship between the calculated adsorption energies, ΔE_O, on $Pd_3M(111)$ surface and the calculated d-band center, $\Delta\varepsilon_d$, in which $\Delta E_O = E^{O}_{alloy} - E^{O}_{Pt}$, $\Delta\varepsilon_d = \varepsilon_d(Pd_3M) - \varepsilon_d(Pd)$.

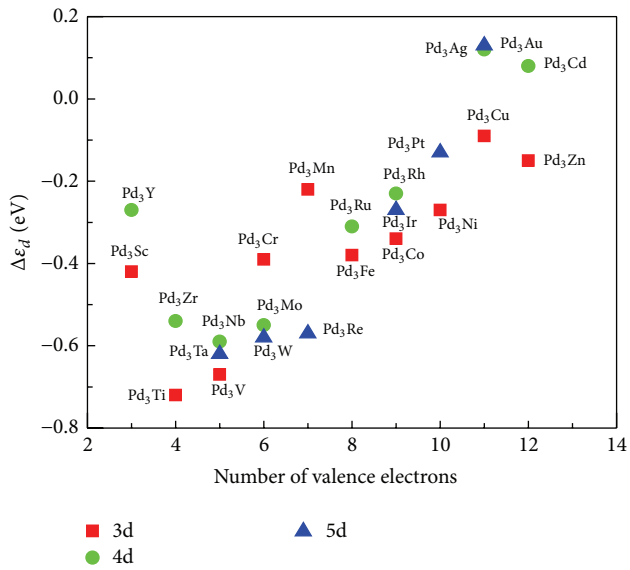

FIGURE 7: The relationship between the calculated d-band center, ε_d, and number of valence electrons in M, $\Delta\varepsilon_d = \varepsilon_d(Pd_3M) - \varepsilon_d(Pd)$.

center, ε_d. However, some alloys such as Pd_3Sc, Pd_3Y, Pd_3Zr, Pd_3Nb, and Pd_3Ta even cause downshift of d-band center, ε_d, although they have larger lattice constants than pure Pd (tensile strain). Therefore, it can be speculated that ligand effect plays important role in determining the downshift or upshift of d-band center, ε_d, of various Pd-M alloys, and, in some cases, it even can dominate the variation of d-band center. For example, in Pd_3Sc, Pd_3Y, Pd_3Zr, Pd_3Nb, and Pd_3Ta alloys, the downshift of d-band center, ε_d, due to the ligand effect is much beyond the upshift caused by lattice expansion.

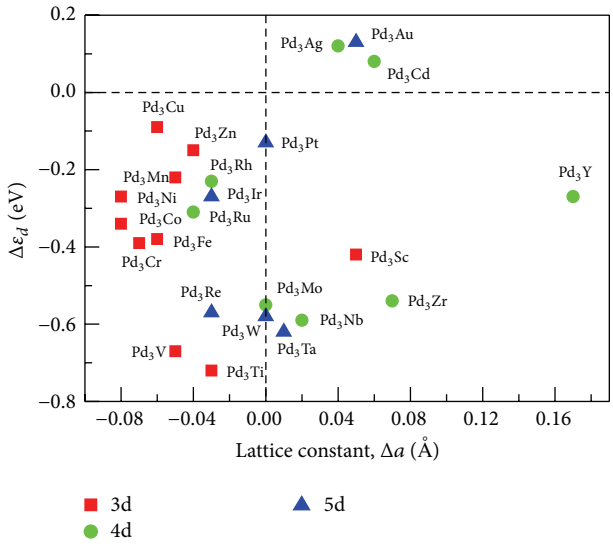

Figure 8: The DFT-calculated d-band center (ε_d) values for the Pd segregated surface as a function of the optimized lattice constant (a) values, in which $\Delta\varepsilon_d = \varepsilon_d(Pd_3M) - \varepsilon_d(Pd)$, $\Delta a = a(Pd_3M) - a(Pd)$.

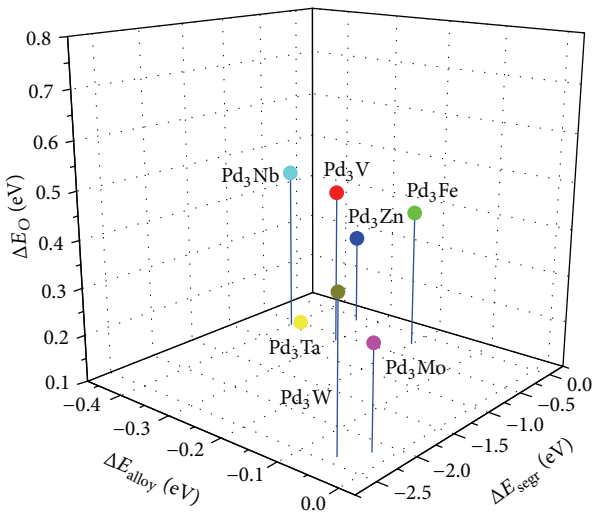

Figure 9: Three-dimensional optimization: high stability and high ORR catalytic activation.

4.3. Screening of Pd-Based Bimetallic Alloy Catalysts. Based on the DFT-calculated results (As shown in Figure 9), Pd-V, Pd-Fe, Pd-Zn, Pd-Nb, Pd-Mo, Pt-Ta, and Pt-W alloys can meet simultaneously three criteria of design of ORR catalysts; that is, $\Delta E_{alloy} < 0$, $\Delta E_{segr} < 0$, and $\Delta E_O > 0$, and the ΔE_O values are within 0.50 eV. However, the formation energy of Pd-Mo and Pd-W alloys is nearly 0; thus, the stability of these two alloys may be relatively poor. The fact that Pd_3Fe have excellent ORR catalytic activity has been reported experimentally [29], which indicated that these three criteria based on DFT calculations are feasible in design of ORR catalysts of Pd-based alloys. The ORR catalytic property of Pd-V, Pd-Zn, Pd-Nb, and Pd-Ta alloys is rarely reported experimentally, and we think that Pd-V, Pd-Zn, Pd-Nb, and Pd-Ta alloys as ORR electrocatalysts in PEMFCs deserve further careful study in the future. In the recent experimental studies by Adzic et al. [27, 39, 40], Pd-Co bimetallic catalyst was found to have enhanced ORR electrocatalytic activity than pure Pt. Based on the ΔE_{segr} value obtained in the present study, Pd-Co alloy can form a stable Pd surface segregated structure because Co has smaller atomic radius and larger surface energy than Pd. However, according to the ΔE_{alloy} value obtained here, the Pd-Co alloy may have problems in forming stable Pd-Co alloy due to slightly positive ΔE_{alloy} value.

5. Conclusions

Developing catalysts for ORR with low noble metal contents, high catalytic activity, and high stability is the key for large-scale application of PEMFCs. We have proposed a multiple-descriptor strategy for rational design of efficient and durable ORR alloy catalysts with low precious metal content based on DFT calculations. We argued that good Pd-based bimetallic catalysts for ORR should simultaneously have negative alloy formation energy, negative surface segregation energy of Pd, and lower oxygen binding strength than pure Pt. By performing detailed DFT calculations on the thermodynamics, surface chemistry, and electronic properties of Pd-M alloys (M is 3d, 4d, and 5d transition metals), Pd-V, Pd-Fe, Pd-Zn, Pd-Nb, and Pd-Ta alloys were identified theoretically to have stable Pd segregated surface and improved ORR activity, among which Pd-Fe alloy has indeed been reported to have excellent ORR catalytic activity. Pd-V, Pd-Zn, Pd-Nb, and Pd-Ta alloys as ORR electrocatalysts in PEMFCs deserve further experimental study in future.

Factors affecting these properties are analyzed carefully. The alloy formation energy ΔE_{alloy} of Pd with transition metals M can be mainly determined by their electron interaction, which makes ΔE_{alloy} values of the most of Pd-M alloys negative due to the large difference in electronegativity except for those in which the alloying transition metals have valence electrons numbers close to Pd. This may be the origin of the negative ΔE_{alloy} for Pd-M alloys. The surface segregation energy of Pd is primarily determined by the surface energy and the atomic radius of M. The metals M which have smaller atomic radius and higher surface energy would tend to favor the surface segregation of Pd in corresponding Pd-M alloys. In some cases, atomic radius can determine the direction of surface segregation of Pd. For instance, Pd-Ti, Pd-Cu, and Pd-Zn alloys, in which Ti possesses a much slight larger atomic radius than Pd, are still predicted to have positive segregation energy of Pd although its slightly higher surface energies than Pd, Cu, and Zn possess much smaller atomic radii than Pd and are still predicted to have a slight trend of Pd surface segregation, in spite of their very low E_{surf} relative to that of Pd. Noticeably, although metal Cr has higher surface energy and lower atomic radius than Pd, Pd_3Cr alloy has positive segregation energy of Pd, indicating that electronic interaction may play the major role in determining the segregation energy of Pd in Pd_3Cr alloy.

The calculated oxygen adsorption energy on the Pd segregated surface roughly linearly correlated with the calculated d-band center of surface Pd atoms. Alloying elements M affect the d-band center by strain effect and ligand effect. Compressive strain generally causes downshift of d-band center, and tensile strain leads to upshift of d-band center. However, Pd_3Sc, Pd_3Y, Pd_3Zr, Pd_3Nb, and Pd_3Ta alloys exhibit downshift of d-band center although they have larger lattice constants than pure Pd, indicating that ligand effect can dominate the variation of d-band center of surface Pd atoms in some cases. In these five alloys, the downshift of d-band center due to ligand effect is much beyond the upshift caused by lattice expansion.

Conflict of Interests

The author declares that they have no conflict of interests.

Acknowledgments

This work is financially supported by National Natural Science Foundation of China (Grant no. 21303048), Hunan Provincial Natural Science Foundation of China (Grant no. 13JJ4101), the Construct Program of the Key Discipline in Hunan Province (Applied Chemistry), and Doctoral Start-up Fund of Hunan University of Arts and Science.

References

[1] C. Wang, N. M. Markovic, and V. R. Stamenkovic, "Advanced platinum alloy electrocatalysts for the oxygen reduction reaction," *ACS Catalysis*, vol. 2, no. 5, pp. 891–898, 2012.

[2] F. Tao, M. E. Grass, Y. Zhang et al., "Evolution of structure and chemistry of bimetallic nanoparticle catalysts under reaction conditions," *Journal of the American Chemical Society*, vol. 132, no. 25, pp. 8697–8703, 2010.

[3] J. Greeley and M. Mavrikakis, "Alloy catalysts designed from first principles," *Nature Materials*, vol. 3, no. 11, pp. 810–815, 2004.

[4] V. R. Stamenkovic, B. S. Mun, M. Arenz et al., "Trends in electrocatalysis on extended and nanoscale Pt-bimetallic alloy surfaces," *Nature Materials*, vol. 6, no. 3, pp. 241–247, 2007.

[5] P. Strasser, S. Koh, T. Anniyev et al., "Lattice-strain control of the activity in dealloyed core—shell fuel cell catalysts," *Nature Chemistry*, vol. 2, no. 6, pp. 454–460, 2010.

[6] T. Toda, H. Igarashi, H. Uchida, and M. Watanabe, "Enhancement of the electroreduction of oxygen on Pt alloys with Fe, Ni, and Co," *Journal of the Electrochemical Society*, vol. 146, no. 10, pp. 3750–3756, 1999.

[7] W. Z. Li, Z. W. Chen, L. B. Xu, and Y. S. Yan, "A solution-phase synthesis method to highly active Pt-Co/C electrocatalysts for proton exchange membrane fuel cell," *Journal of Power Sources*, vol. 195, no. 9, pp. 2534–2540, 2010.

[8] V. R. Stamenkovic, B. Fowler, B. S. Mun et al., "Improved oxygen reduction activity on $Pt_3Ni(111)$ via increased surface site availability," *Science*, vol. 315, no. 5811, pp. 493–497, 2007.

[9] S. Koh and P. Strasser, "Electrocatalysis on bimetallic surfaces: modifying catalytic reactivity for oxygen reduction by voltammetric surface dealloying," *Journal of the American Chemical Society*, vol. 129, no. 42, pp. 12624–12625, 2007.

[10] S. Chen, W. C. Sheng, N. Yabuuchi, P. J. Ferreira, L. F. Allard, and Y. Shao-Horn, "Origin of oxygen reduction reaction activity on 'Pt_3Co' nanoparticles: atomically resolved chemical compositions and structures," *Journal of Physical Chemistry C*, vol. 113, no. 3, pp. 1109–1125, 2009.

[11] M. Wakisaka, H. Suzuki, S. Mitsui, H. Uchida, and M. Watanabe, "Increased oxygen coverage at Pt-Fe alloy cathode for the enhanced oxygen reduction reaction studied by EC-XPS," *Journal of Physical Chemistry C*, vol. 112, no. 7, pp. 2750–2755, 2008.

[12] V. Stamenkovic, B. S. Mun, K. J. J. Mayrhofer et al., "Changing the activity of electrocatalysts for oxygen reduction by tuning the surface electronic structure," *Angewandte Chemie International Edition*, vol. 45, no. 18, pp. 2897–2901, 2006.

[13] U. A. Paulus, A. Wokaun, G. G. Scherer et al., "Oxygen reduction on carbon-supported Pt-Ni and Pt-Co alloy catalysts," *Journal of Physical Chemistry B*, vol. 106, no. 16, pp. 4181–4191, 2002.

[14] S. Koh, J. Leisch, M. F. Toney, and P. Strasser, "Structure-activity-stability relationships of Pt-Co alloy electrocatalysts in gas-diffusion electrode layers," *Journal of Physical Chemistry C*, vol. 111, no. 9, pp. 3744–3752, 2007.

[15] H. A. Gasteiger, S. S. Kocha, B. Sompalli, and F. T. Wagner, "Activity benchmarks and requirements for Pt, Pt-alloy, and non-Pt oxygen reduction catalysts for PEMFCs," *Applied Catalysis B: Environmental*, vol. 56, no. 1-2, pp. 9–35, 2005.

[16] C. Wang, M. Chi, D. Li et al., "Synthesis of homogeneous Pt-bimetallic nanoparticles as highly efficient electrocatalysts," *ACS Catalysis*, vol. 1, no. 10, pp. 1355–1359, 2011.

[17] A. S. Aricó, A. Stassi, I. Gatto, G. Monforte, E. Passalacqua, and V. Antonucci, "Surface properties of Pt and PtCo electrocatalysts and their influence on the performance and degradation of high-temperature polymer electrolyte fuel cells," *Journal of Physical Chemistry C*, vol. 114, no. 37, pp. 15823–15836, 2010.

[18] K. Matsutani, T. Tada, and K. Hayakawa, "Effect of particle size of platinum and platinum-cobalt catalysts on stability against load cycling," *Platinum Metals Review*, vol. 54, no. 4, pp. 223–232, 2010.

[19] P. Yu, M. Pemberton, and P. Plasse, "PtCo/C cathode catalyst for improved durability in PEMFCs," *Journal of Power Sources*, vol. 144, no. 1, pp. 11–20, 2005.

[20] N. Wakabayashi, M. Takeichi, H. Uchida, and M. Watanabe, "Temperature dependence of oxygen reduction activity at Pt–Fe, Pt–Co, and Pt–Ni alloy electrodes," *Journal of Physical Chemistry B*, vol. 109, no. 12, pp. 5836–5841, 2005.

[21] R. Loukrakpam, J. Luo, T. He et al., "Nanoengineered PtCo and PtNi catalysts for oxygen reduction reaction: an assessment of the structural and electrocatalytic properties," *Journal of Physical Chemistry C*, vol. 115, no. 5, pp. 1682–1694, 2011.

[22] P. Mani, R. Srivastava, and P. Strasser, "Dealloyed binary PtM3 (M = Cu, Co, Ni) and ternary $PtNi_3M$ (M = Cu, Co, Fe, Cr) electrocatalysts for the oxygen reduction reaction: performance in polymer electrolyte membrane fuel cells," *Journal of Power Sources*, vol. 196, no. 2, pp. 666–673, 2011.

[23] O. Savadogo, K. Lee, K. Oishi, S. Mitsushima, N. Kamiya, and K. I. Ota, "New palladium alloys catalyst for the oxygen reduction reaction in an acid medium," *Electrochemistry Communications*, vol. 6, no. 2, pp. 105–109, 2004.

[24] V. Raghuveer, A. Manthiram, and A. J. Bard, "Pd–Co–Mo electrocatalyst for the oxygen reduction reaction in proton exchange membrane fuel cells," *Journal of Physical Chemistry B*, vol. 109, no. 48, pp. 22909–22912, 2005.

[25] M. H. Shao, T. Huang, P. Liu et al., "Palladium monolayer and palladium alloy electrocatalysts for oxygen reduction," *Langmuir*, vol. 22, no. 25, pp. 10409–10415, 2006.

[26] K. Lee, O. Savadogo, A. Ishihara, S. Mitsushima, N. Kamiya, and K. I. Ota, "Methanol-tolerant oxygen reduction electrocatalysts based on Pd-3D transition metal alloys for direct methanol fuel cells," *Journal of the Electrochemical Society*, vol. 153, no. 1, pp. A20–A24, 2006.

[27] L. Zhang, K. Lee, and J. Zhang, "The effect of heat treatment on nanoparticle size and ORR activity for carbon-supported Pd-Co alloy electrocatalysts," *Electrochimica Acta*, vol. 52, no. 9, pp. 3088–3094, 2007.

[28] R. R. Adzic, "Palladium-cobalt particles as oxygen-reduction electrocatalysts," in *Proceedings of the DOE Hydrogen, Fuel Cell & Infrastructure Technologies Program Review Meeting*, Philadelphia, Pa, USA, 2004.

[29] M. H. Shao, K. Sasaki, and R. R. Adzic, "Pd–Fe nanoparticles as electrocatalysts for oxygen reduction," *Journal of the American Chemical Society*, vol. 128, no. 11, pp. 3526–3527, 2006.

[30] J. L. Fernández, D. A. Walsh, and A. J. Bard, "Thermodynamic guidelines for the design of bimetallic catalysts for oxygen electroreduction and rapid screening by scanning electrochemical microscopy. M-Co (M: Pd, Ag, Au)," *Journal of the American Chemical Society*, vol. 127, no. 1, pp. 357–365, 2005.

[31] S. Guerin, B. E. Hayden, C. E. Lee et al., "Combinatorial electrochemical screening of fuel cell electrocatalysts," *Journal of Combinatorial Chemistry*, vol. 6, no. 1, pp. 149–158, 2004.

[32] J. Greeley, J. K. Nørskov, and M. Mavrikakis, "Electronic structure and catalysis on metal surfaces," *Annual Review of Physical Chemistry*, vol. 53, pp. 319–348, 2002.

[33] J. L. Fernández, V. Raghuveer, A. Manthiram, and A. J. Bard, "Pd-Ti and Pd-Co-Au electrocatalysts as a replacement for platinum for oxygen reduction in proton exchange membrane fuel cells," *Journal of the American Chemical Society*, vol. 127, no. 38, pp. 13100–13101, 2005.

[34] J. L. Fernández, J. Michael White, Y. Sun, W. Tang, G. Henkelman, and A. J. Bard, "Characterization and theory of electrocatalysts based on scanning electrochemical microscopy screening methods," *Langmuir*, vol. 22, no. 25, pp. 10426–10431, 2006.

[35] Y. X. Wang and P. B. Balbuena, "Design of oxygen reduction bimetallic catalysts: ab-initio-derived thermodynamic guidelines," *Journal of Physical Chemistry B*, vol. 109, no. 40, pp. 18902–18906, 2005.

[36] Y. Wang and P. B. Balbuena, "Potential energy surface profile of the oxygen reduction reaction on a Pt cluster:adsorption and decomposition of OOH and H_2O_2," *Journal of Chemical Theory and Computation*, vol. 1, no. 5, pp. 935–943, 2005.

[37] M. R. Tarasevich, G. V. Zhutaeva, V. A. Bogdanovskaya, M. V. Radina, M. R. Ehrenburg, and A. E. Chalykh, "Oxygen kinetics and mechanism at electrocatalysts on the base of palladium-iron system," *Electrochimica Acta*, vol. 52, no. 15, pp. 5108–5118, 2007.

[38] E. J. Lamas and P. B. Balbuena, "Oxygen reduction on $Pd_{0.75}Co_{0.25}$ (111) and $Pt_{0.75}Co_{0.25}$ (111) surfaces: an ab initio comparative study," *Journal of Chemical Theory and Computation*, vol. 2, no. 5, pp. 1388–1394, 2006.

[39] M. Shao, P. Liu, J. Zhang, and R. R. Adzic, "Origin of enhanced activity in palladium alloy electrocatalysts for oxygen reduction reaction," *Journal of Physical Chemistry B*, vol. 111, no. 24, pp. 6772–6775, 2007.

[40] Y. Suo, L. Zhuang, and J. Lu, "First-principles considerations in the design of Pd-alloy catalysts for oxygen reduction," *Angewandte Chemie International Edition*, vol. 46, no. 16, pp. 2862–2864, 2007.

[41] V. R. Stamenkovic, B. S. Mun, K. J. J. Mayrhofer, P. N. Ross, and N. M. Markovic, "Effect of surface composition on electronic structure, stability, and electrocatalytic properties of Pt-transition metal alloys: Pt-skin versus Pt-skeleton surfaces," *Journal of the American Chemical Society*, vol. 128, no. 27, pp. 8813–8819, 2006.

[42] J. L. Zhang, M. B. Vukmirovic, K. Sasaki, A. U. Nilekar, M. Mavrikakis, and R. R. Adzic, "Mixed-metal Pt monolayer electrocatalysts for enhanced oxygen reduction kinetics," *Journal of the American Chemical Society*, vol. 127, no. 36, pp. 12480–12481, 2005.

[43] S. R. Calvo and P. B. Balbuena, "Theoretical analysis of reactivity on Pt(1 1 1) and Pt–Pd(1 1 1) alloys," *Surface Science*, vol. 601, no. 1, pp. 4786–4792, 2007.

[44] J. K. Nørskov, J. Rossmeisl, A. Logadottir et al., "Origin of the overpotential for oxygen reduction at a fuel cell cathode," *Journal of Physical Chemistry B*, vol. 108, no. 46, pp. 17886–17892, 2004.

[45] J. P. Perdew, K. Burke, and M. Ernzerhof, "Generalized gradient approximation made simple," *Physical Review Letters*, vol. 77, no. 18, pp. 3865–3868, 1996.

[46] D. Vanderbilt, "Soft self-consistent pseudopotentials in a generalized eigenvalue formalism," *Physical Review B*, vol. 41, no. 11, pp. 7892–7895, 1990.

[47] M. Methfessel and A. T. Paxton, "High-precision sampling for Brillouin-zone integration in metals," *Physical Review B*, vol. 40, no. 6, pp. 3616–3621, 1989.

[48] S. Baroni, A. Dal Corso, S. de Gironcoli, and P. Giannozzi, PWSCF and PHONON: plane-wave pseudo-potential codes, 2001, http://www.pwscf.org/.

[49] A. Kokalj, "XCrySDen—a new program for displaying crystalline structures and electron densities," *Journal of Molecular Graphics and Modelling*, vol. 17, no. 3-4, pp. 176–179, 1999.

[50] A. Kokalj and M. Causa, "Scientific visualization in computational quantum chemistry," in *Proceedings of the High Performance Graphics Systems and Applications European Workshop*, CINECA-Interuniversity Consortium, Bologna, Italy, 2000.

[51] A. Kokalj and M. Causà, XCrySDen: [X-Window] CRYstalline Structures and DENsities, 2001, http://www.xcrysden.org/.

[52] S. Mukerjee, S. Srinivasan, and M. P. Soriaga, "Role of structural and electronic properties of Pt and Pt alloys on electrocatalysis of oxygen reduction," *Journal of the Electrochemical Society*, vol. 142, no. 5, pp. 1409–1422, 1995.

[53] B. Hammer and J. K. Nørskov, "Electronic factors determining the reactivity of metal surfaces," *Surface Science*, vol. 343, no. 3, pp. 211–220, 1995.

[54] B. Hammer and J. K. Norskov, "Why gold is the noblest of all the metals," *Nature*, vol. 376, no. 6537, pp. 238–240, 1995.

[55] L. H. Ou and S. L. Chen, "Comparative study of oxygen reduction reaction mechanisms on the Pd(111) and Pt(111) surfaces in acid medium by DFT," *Journal of Physical Chemistry C*, vol. 117, no. 3, pp. 1342–1349, 2013.

[56] J. Greeley, I. E. L. Stephens, A. S. Bondarenko et al., "Alloys of platinum and early transition metals as oxygen reduction electrocatalysts," *Nature Chemistry*, vol. 1, no. 7, pp. 552–556, 2009.

[57] A. Peter and L. Jones, *Chemistry: Molecules, Matter and Change*, W. H. Freeman, New York, NY, USA, 1997.

[58] O. M. Løvvik, "Surface segregation in palladium based alloys from density-functional calculations," *Surface Science*, vol. 583, no. 1, pp. 100–106, 2005.

[59] J. K. Nørskov, T. Bligaard, A. Logadottir et al., "Universality in heterogeneous catalysis," *Journal of Catalysis*, vol. 209, no. 2, pp. 275–278, 2002.

[60] N. L. Allinger, X. Zhou, and J. Bergsma, "Molecular mechanics parameters," *Journal of Molecular Structure: THEOCHEM*, vol. 312, no. 1, pp. 69–83, 1994.

[61] F. R. De Boer, R. Boom, W. C. M. Mattens, A. R. Miedema, and A. K. Niessen, *Cohesion in Metals*, North-Holland Publishing, Amsterdam, The Netherlands, 1988.

[62] G. E. Ramírez-Caballero, Y. Ma, R. Callejas-Tovar, and P. B. Balbuena, "Surface segregation and stability of core-shell alloy catalysts for oxygen reduction in acid medium," *Physical Chemistry Chemical Physics*, vol. 12, no. 9, pp. 2209–2218, 2010.